Chaotic Dynamics of RLD Oscillator

Abstract

Chaos is aperiodic behavior in deterministic nonlinear dynamical systems that is highly sensitive to initial conditions. Chaotic behavior can be observed in a simple electronic (RLD) circuit consisting of a resistor, diode, and inductor with an oscillatory voltage drive signal. The output voltage signal exhibits both stable periodic behavior and chaotic behavior, which are visualized by power spectra and phase diagrams. False nearest neighbor analysis is used to elucidate the dimensionality of a system, distinguishing between chaos and noise. Synchronized chaotic circuits can be useful for secure communication applications.

Micah Richert
Diane Whitmer
June 13, 2003
Biophysical Measurements Lab

Table of Contents

Introduction

Chaos is a class of complex behaviors that can emerge from nonlinear dynamical systems, and is ubiquitous both in the natural world and technology. Many biological systems such as the human heart and invertebrate neurons naturally exhibit chaotic behavior. Furthermore, digital computing has made feasible the creation of fractal patterns based on chaos. The beauty of chaos, however, lies not in the aesthetic of fractals, but in the simplicity of the system from which such complex, unpredictable behavior can emerge.

The electronic RLD circuit is one example of a simple system that can exhibit chaotic behavior. Building a chaotic circuit is a useful aid for understanding the mathematics and applications of this pervasive phenomenon.

Chaos lies in the middle of a spectrum that many people conceptualize as a dichotomy between signal and noise; it is in practical terms a signal that appears noisy, but for which this "noise" has structure and meaning. Chaos is a specific type of nonlinear dynamical system, one that is aperiodic, non-repeatable, and highly sensitive to initial conditions. Many data analysis techniques, such as spectral analysis, hinge upon an assumption of linearity, and strive to average out fluctuations believed to be noise. A different set of techniques is required for nonlinear systems, in which averaging out fluctuations would mean the throwing away of information about the dynamics of the system. When the underlying dynamics of a system is not known, analysis tools created for understanding chaotic systems can be used to determine whether a system is noisy or chaotic. Specifically, phase space reconstruction can reveal the dimensionality of the underlying data, and suggest the number of equations necessary to describe the system.

Chaos is not only useful for data analysis, but has broad application in technology. For example, pacemakers for the heart could incorporate chaotic dynamics to more closely resemble the natural behavior of the heart. Furthermore, chaotic signals can be used as an encryption technique for communication.

This lab project consists of building a chaotic circuit, analyzing the circuit itself, analyzing chaotic data from the circuit, and an attempt at building of a secure communication system.

Motivation

In 1997 M. Feigenbaum published a seminal paper proving that if a system exhibits repeated period doubling by increasing some finite parameter, then the system will have an infinite number of period doublings or bifurcations in a finite increase of that parameter (Feigenbaum, 1977). This idea is expressed by the following recursive equation:

$$x_{n+1} = r\, x_n(1 - x_n)$$

The logistic map is a simple example of a system that demonstrates this phenomenon (figure 1).
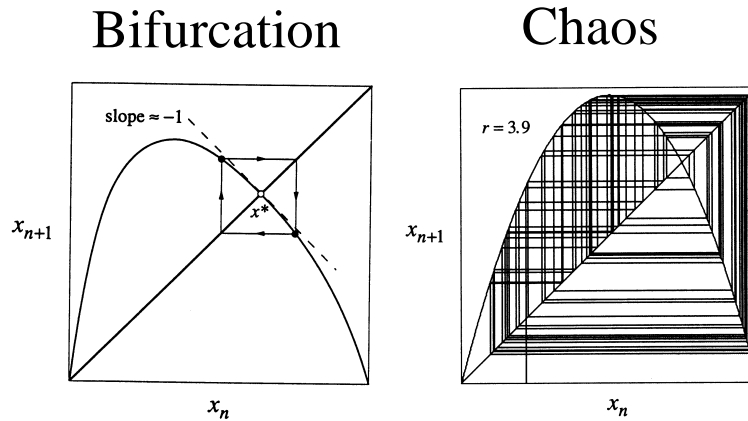
Bifurcation   Chaos

Figure 1. Comparison between Bifurcation and Chaos in the Logistic Map.
(Strogatz, 1994, pp .360 & 355.)

The logistic map is an equation used to model population dynamics. The variable r is a scaling factor, and as r is increased the properties of the logistic map changes. Shown above is a bifurcation for an r slightly above 1; the circles are stable points. For values of r less than 1, there is only one stable point. The system effectively alternates between one point and the other, and all other points eventually converge to this 2-point limit cycle. For the chaotic illustration, r = 3.9, and if one starts from an arbitrary point in the system, the system will result in a non-repeating series of points with no apparent pattern.

A very simple electronic system that exhibits this period doubling route to chaos is the chaotic resonator, first demonstrated in 1981 by Paul S. Linsay. This circuit is made of three basic components in series: a resistor, diode and inductor.

This circuit can then be used to investigate the control of chaos, and in particular synchronization of chaos. Using a continuous unidirectional proportional feedback, one can control a slave oscillator by synchronizing it to the master; this was first demonstrated by Newell et al in 1993, and later revised by Mozdy et al in 1995.

Previous work on this circuit from a couple of class projects at Harvard University, has entailed investigating the effect of increasing the amount of noise in the circuit and the bifurcation points (Greene et al., unpublished), and demonstrating that this system has the expected Feigenbaum universal constant (Schaffer et al, unpublished).

Period Doubling Route to Chaos

Period doubling as a route to chaos is address in general mathematical terms by Feigenbaum. He proves that if the system exhibits period doubling by increasing a single parameter, then the system has a universal constant $\delta = 4.669...$ Such that

$$\delta = \lim_{n \to \infty} \frac{b_{n+1} - b_n}{b_{n+2} - b_{n+1}},$$

where b_n is the parameter value at which the nth bifurcation occurred. A bifurcation is also known as a period doubling.

In the chaotic resonator circuit, the circuit undergoes pitchfork bifurcation as the peak-to-peak drive voltage is increased, and is evident by the appearance and a new frequency component at half the drive frequency. As the amplitude is further increased, the bifurcated signal bifurcates again. The amplitude at which each

bifurcation occurs decreases geometrically according to the Feigenbaum equation. This progression iterates until there are an infinite number of bifurcations from a finite increase of drive voltage, resulting in chaos.

The phase diagram depicted in figure 2 demonstrates this bifurcation process. In phase space, an ordinary resonator circuit would be a single orbit, which is what the output of the circuit looks like for low drive amplitudes. As the amplitude is increased, a new frequency component appears, and this new frequency results in seeing two orbits in the phase space plot. Unfortunately, the amplitude of the period doubled frequency, as well as all other bifurcation frequencies, is extremely low. To be able to visualize the bifurcations, as well as chaos, one must zoom in to the phase space plot to the point where one can no longer see the entire orbit, but instead see only a very small slice.
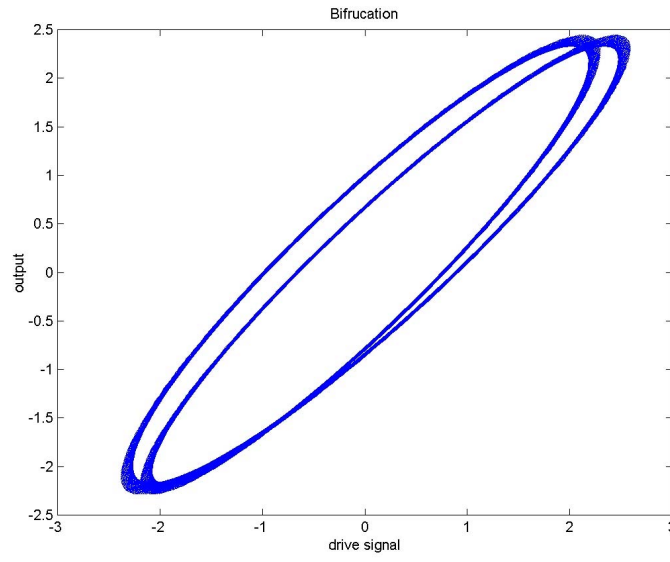
Figure 2.
Phase Plot of Bifurcation: Output signal as a function of drive signal.

How to Build a Chaotic Circuit

Overview

The circuit required to create chaos is simple to build, and consists of a small resistor, large inductor and a diode in series. Figure 3 illustrates the schematic for this circuit.
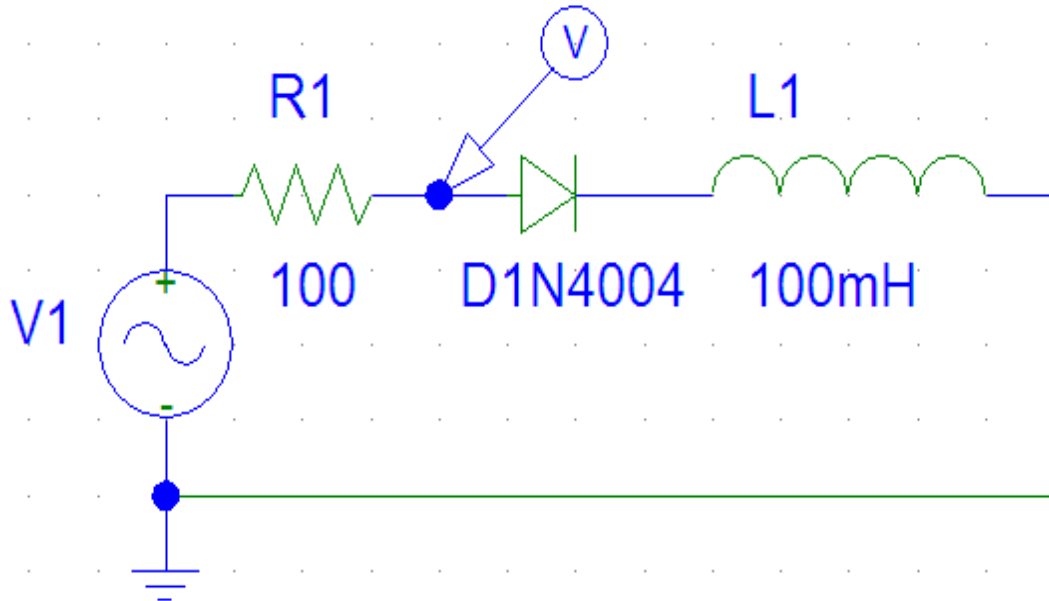
Figure 3. Simple Chaotic Circuit

The signal supplied to drive the circuit is a sinusoid with variable peak-to-peak amplitude. For most of our experiments, we used a 10 Volt peak-to-peak auditory oscillator set to 20 KHz. We chose an audio oscillator over a digital function generator because the synthesized sine waves produced by digital function generators can be noisy. Reduction of noise sources is critical for studying a chaotic circuit.

As the circuit is driven with higher peak-to-peak amplitudes, the circuit takes on nonlinear behavior. Namely, this circuit exhibits a period doubling route to chaos. Voltage was measured between the resistor and diode relative to ground.

The circuit is a modification of the prototypical RLC circuit, but with the capacitor replaced by the diode. The diode can then be modeled as an ideal diode and a voltage dependent capacitance, as depicted below:
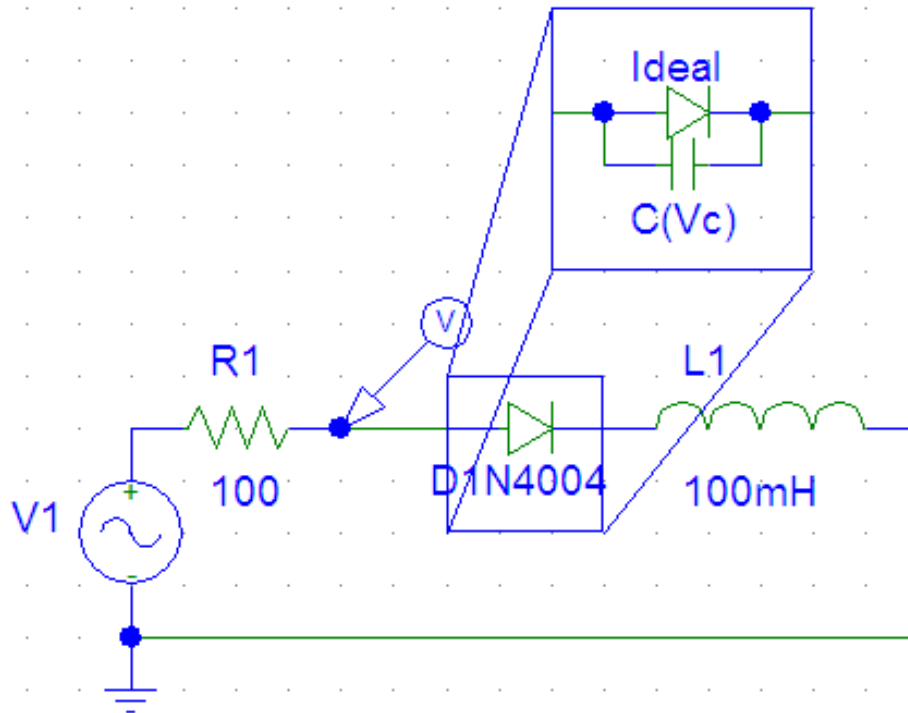
Figure 4. Ideal Diode and Voltage Dependent Capacitance as Model for Circuit.

Building the circuit

As discussed earlier, the simple resonator circuit is composed of a resistor, diode and inductor all in series, with a sinusoidal drive voltage. The components were chosen to exhibit chaos at a relatively low frequency. The frequency where chaos is possible is approximately

$$f = \frac{1}{2\pi\sqrt{LC}},$$

where L is the inductance and C is the approximate capacitance of the diode. Since the diode is not changed (always an N4004) and the capacitance is fixed, the inductor must be large for the resonance frequency be low. This is why we chose a 100 mH inductor. A 100 Ohm resistor was chosen because the resistor effectively sets the bandwidth of the resonator, and therefore should be relatively small.

To build the circuit, simply place all 3 components in series in a breadboard and attach the drive. Refer to figure 1 as a guide for properly assembling the components.

The Synchronization Circuit

We also investigated synchronizing two *identical* chaotic resonators. To approximate "identical," we tested and chose pairs of components with the most similar characteristics. We tested the lowest voltage needed for a single bifurcation and the frequency at which this lowest bifurcation occurred. Since we only had five 100mH inductors, we were fairly limited on matching them. However, we had a supply of 500 diodes and sampled well over a hundred before choosing a pair.

The synchronization circuit is composed of two chaotic oscillators as constructed above. Of the two circuits, one is the master, and the other is the slave. Ideally, the slave matches the master. This matching can be confirmed by examination of a phase space diagram of master output versus slave output. When the two circuits are synchronized, this phase plot approaches a straight line.

The chaotic control method used is a continuous version of the Occasional Proportional Feedback (OPF) controller. The basic idea is that if the two systems are relatively similar to begin with, then only small (linear) corrections will be needed in order to keep the slave oscillator matched to the master. To generate the correction signal, the states of the two circuits are compared, and a scaled down version of this difference is added to the slave's drive signal. This correction signal can be thought of as a negative feedback signal, or weak coupling in a coupled oscillator system. The coupling is unidirectional, which means that the master circuit does not have any correction or feedback applied to its drive. The state of the system is measured in the same way the output of the circuit is measured, between the resistor and diode. Note, our circuit varies from that described by Mozdy et al. 1995, both in the order of the components in resonator circuit and in the location from which the voltage is measured.

The required circuits for the unidirectional control are instrumentational amplifier (subtractor), potentiometer (variable resistor), and voltage adder. The instrumentational amplifier is comprised of three opamps. Two opamps act as buffers and the third computes the subtraction. Then this subtracted voltage needs to be scaled down, so that we can have variable gain. Finally, this scaled down voltage is added to the drive voltage. The voltage adder is actually done with a current adder, which has the side effect that the output voltage is inverted; therefore, the voltage needs to be inverted again using a single input current adder.

The circuit that we used is schematically drawn below. We have several more opamps in our circuit than is absolutely necessary; this is because we have found that the phase lag introduced by the opamps is significant. To tackle this problem with phase lag, we added opamps between the drive signal and the master oscillator in order to match the amount of delay between the drive and the slave oscillator. Opamps U1A – U4A are serving this purpose: to match the phase lag. Opamps U19A – U21A are the three opamps that make up the instrumentational amplifier. U16A and U17A are two buffers used to ensure that the correction signal is not contaminated by the drive and to ensure that the third opamp in the instrumentational amplifier does not saturate; these two opamps are probably not needed. U6A is a buffer used to isolate the drive from the slave circuitry. U7A and U8A make up the voltage adder.

The specific opamps we used were ST's TL071CN or TL084CN.

The variable gain for the feed back is accomplished using a voltage divider circuit, with a 10K resister in series with a 10K potentiometer. However, there are several complications with this simple circuit. First, there seems to be a DC bias in the difference signal, which creates an even larger error when it is feedback to the circuit. This larger error then increases the difference signal which has the DC bias applied to it again, and the signal eventually explodes if the gain is too high. To deal with the DC bias, a 47pF capacitor was added between the 10K resistor and the potentiometer. Once the DC bias was successfully controlled for, a resonance developed inside of the feedback loop at approximately 400 KHz. To filter out this high frequency feedback, we added a 471pF capacitor after the 10K resistor to ground.

The gain and filtering circuit that we used is illustrated in the schematic, however, this circuit does not function exactly as described above. The 47pF capacitor needs to be placed between the 10K resistor and

potentiometer and the opamp, for the circuit to work as we described it. However, we did not realize the error until after the synchronization data was collected. It leaves it to be demonstrated that the intended circuit would be better at synchronization than the configuration actually used.

A significant stumbling block that we encountered was that there was an extremely high frequency noise appearing on the master resonator once the opamps were added to the circuit. As it turns out, the power supply's +15,-15 lines, which power the opamps, had small amplitude fluctuations. To remove these fluctuations, two capacitors were added between +15 to ground, and –15 to ground, they are depicted as C3 and C4 in the diagram (figure 5).
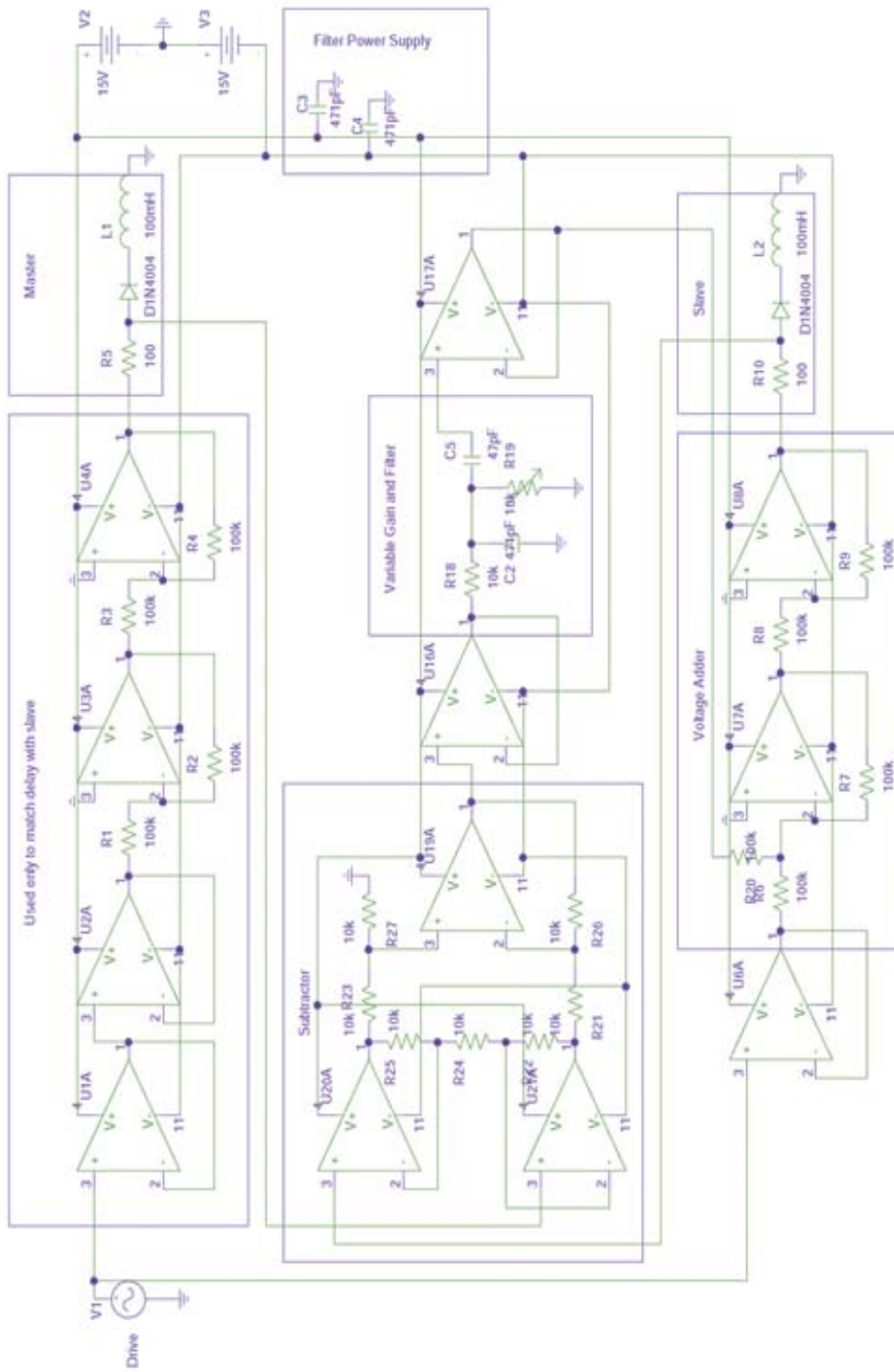
Figure 5. Circuit Diagram of Two Synchronized Oscillator System.

Observations on Circuit Modifications

There are some alternative designs of the circuit worth exploring. The diode can be replaced with an LED, as well as a photodiode. The circuit is believed to exhibit chaos because of the voltage dependent capacitance. Therefore, if a LED or photodiode with a large voltage dependent capacitance can be found, then the diode could be replaced with that component.

One interesting possibility is to optically record the state of the chaotic system with an LED in place of the diode. Several different LEDs were tested to see if chaos or at the least a bifurcation was possible in the 10 Volt peak-to-peak drive amplitude range. Ultra-Bright white, yellow and red LEDs were tested, but none exhibited even a single bifurcation. The Ultra-Brights were tested because they have extremely anomalous properties, one of which might be a large Voltage-dependent capacitance. This still might be the case, but their high resistance effectively makes chaos unachievable. An unknown green LED did bifurcate at approximately 8 Volts, but none of the higher bifurcations were achievable with our function generators.

Another idea for modifying the circuit is to drive the circuit into chaos by changing the internal dynamics of the diode instead of changing the drive amplitude. To be able to change the dynamics of the diode component, replace it with a photodiode. As more or less light is applied to the photodiode, its dynamics change. We tested a single IR photodiode. This photodiode demonstrated chaos at a lower drive voltage than the N4004 diode which we were using, but did not have a significantly lower frequency. What seems counter-intuitive is that as more light is applied to the photodiode, the more chaos was observed. This might be a very interesting phenomenon to investigate further.

Distinguishing Chaos from Noise

Phase Space Embedding and False Nearest Neighbors

As mentioned previously, one of the utilities of chaos is that it can provide a framework for analyzing where on the spectrum between pure signal and pure noise, a data set might fall. Chaos is a type of signal, but can appear to be noise if not analyzed properly. Chaotic signals are irregular in time, but highly structured in phase space. Phase space embedding therefore provides a tool for visualizing the structure of chaotic signals, and for distinguishing chaos from noise. Furthermore, noise, by definition, is infinitely dimensional, whereas chaos is (relatively small) finite dimensional. Time series data can therefore be "unfolded" into higher dimensional space by sampling data points at fixed distances. A new data point will be created from a single time point and some integer number of steps ahead of that time point. For example, a voltage signal at time t: $V(t)$ can be plotted in three-dimensional space as $V(t)$ vs. $V(t + \tau)$ vs. $V(t + 2\tau)$. Embedding theorem proves that a sequential ordering of the points still follows the underlying dynamics (Abarbanel, p.17 and citations therein).

Once time series data is represented in multivariate space, the next step is to find the dimensionality of the underlying dynamics. There is risk in a phase space reconstruction that some points will neighbor on each other because they have been projected into too low of a space from a higher dimension. These points are termed "false nearest neighbors," and can be used as a metric for finding the appropriate dimensionality of the phase space. Specifically, a global nearest neighbors value is calculated based on the average Euclidian distance between each point and its n nearest neighbors, where n is a parameter to be set. A threshold is set such that when the average distance between false nearest neighbors exceeds it, the data is unfolded into the next higher dimensional space. This process is repeated until the global false nearest neighbor distance does not change, at which point the attractor of the system has been revealed.

One of the challenges of using the false nearest neighbor method lies in the choosing of the time lag τ. Although there is not a mathematical formalism for determining these parameters, there are guidelines. By necessity, τ will be some multiple of the sampling rate of the data, given that the data is already discretized. τ must also be large enough to change significantly between time steps and display the underlying dynamics of the system, but not so large that it is unstable. (Remember that chaotic systems, by definition, are sensitive to initial conditions and neighboring points separate exponentially in time.) A useful heuristic for determining τ is to calculate the average mutual information and use the time lag at which the first minimum occurs as the intitial τ (Abarbanel, 1996). Mutual information is a theoretical construct that describes how interdependent two measurements are with each other. When the mutual information is a minimum, the two measurements are fairly independent of each other, but not so independent that there is no connection. This makes for a useful time delay τ such that it is connected with the nonlinear information that describes the underlying dynamics of the system. An alternative to choosing T based on the first minimum of average mutual information is to choose the first zero crossing of the linear autocorrelation function of the data.

The goal of false nearest neighbors analysis is to determine the dimensionality of the data and to plot the attractor. CSPW (1996) is a software package that computes the dimensionality based on the process described above, iterating through a number of false nearest neighbor calculations. This software was used for the analysis of circuit data.

Results

Analysis of Period Doubling

Our first set of data collected was used to test the circuit for period doubling behavior on the route to chaos. We drove our initial circuit, which was constructed with a 3.4 mH inductor, with a 150 kHz sinusoid at various amplitudes. Using an output versus input (x-y) plot on the oscilloscope, we judged by eye when the circuit bifurcated by counting the number of orbits. Furthermore, we judged chaos by the appearance of the orbits turning fuzzy, with an uncountable (infinite) number of orbits.

At a drive amplitude of 0.542 to 0.659 Volts, one route to chaos was observed and is plotted as the first four bars in the bar chart below (figure 6). A second route to chaos was observed between 0.74 and 1.658 Volts (figure 6). A height greater than 40 in the bar chart represents an uncountable number of orbits, which is the signature of chaos.
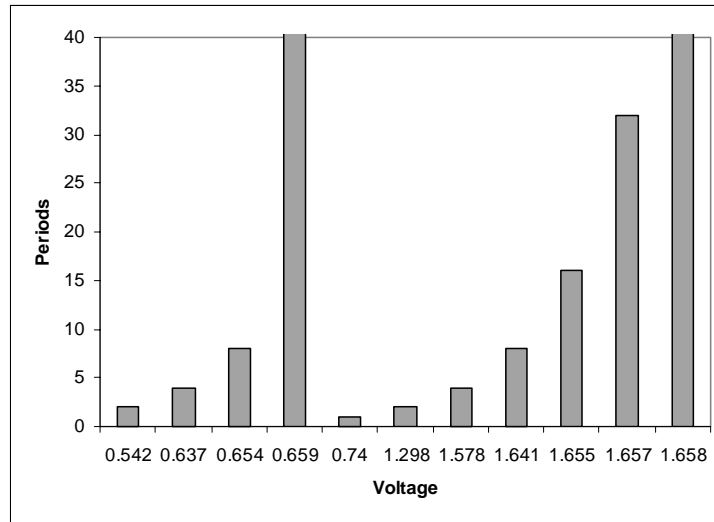
Figure 6. Route to Chaos.

We used this data to calculate the universal δ constant based on Feigenmaum's theory. The universal constant measured from these voltages is 5.58 and 4.44 for the two routes to chaos shown, as compared to $\delta = 4.669$ measured by Feigenbaum. These values were not only the right order of magnitude, but surprisingly close to the Feigenbaum constant.

As demonstrated by the data, there are two ranges where chaos is possible from a single orbit, this has never been published but has been seen by other researchers. We observed that for voltages significantly higher than 1.7 volts, stable orbits higher than 2-cycle orbits exist on the period-doubling path to chaos. We observed both a 3-cycle orbit on a period doubling route to chaos, and 5-cycle stable orbit on the path to chaos at higher voltages (not shown here).

Time Series Data from Simple Circuit

Our next set of data is taken from the improved circuit (described in "Building the Circuit") during 2-second traces, sampled at 200 kHz. In the next few sections, we analyze these data in detail. The following traces are 5 msec and 0.5 msec segments from a baseline voltage measurement.
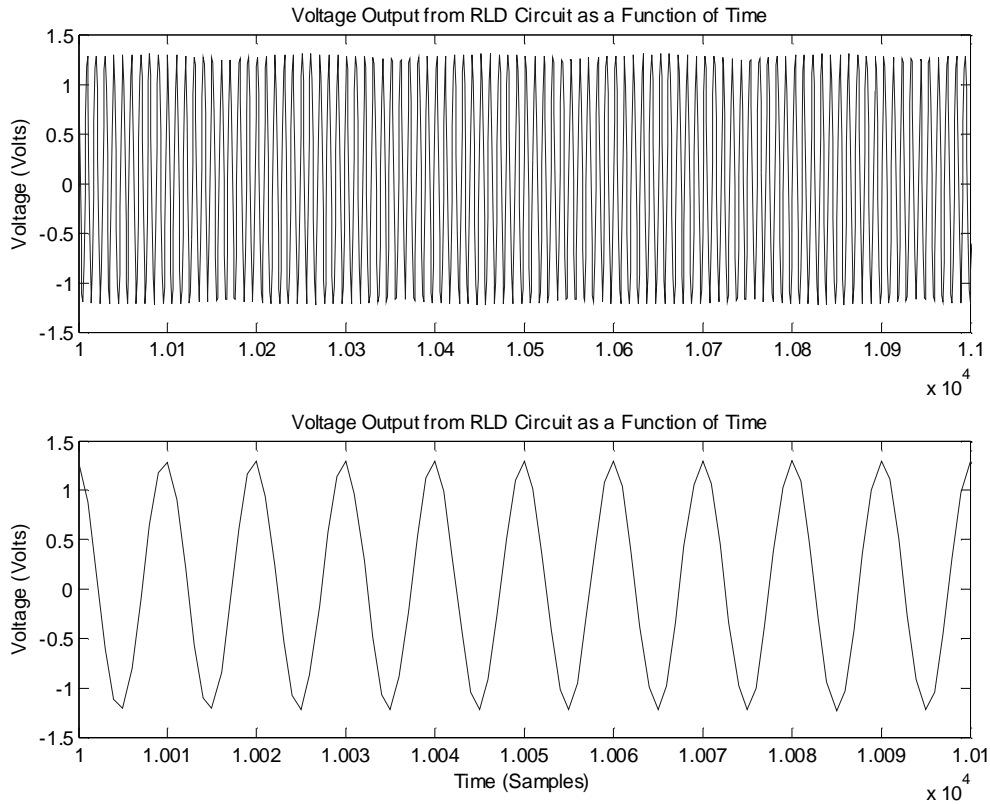
Figure 7.
Baseline Measurement. Drive signal: 3V (peak to peak), 20 kHz sine wave.
1 sample = 0.005 msec

As these data show, the 20 kHz drive frequency dominates the signal, and the signal of interest is on the order of milliVolt changes on top of 5 to 10 Volt drive signal. These perturbations are perhaps more obvious in the time trace from a chaotic signal (figure 8).
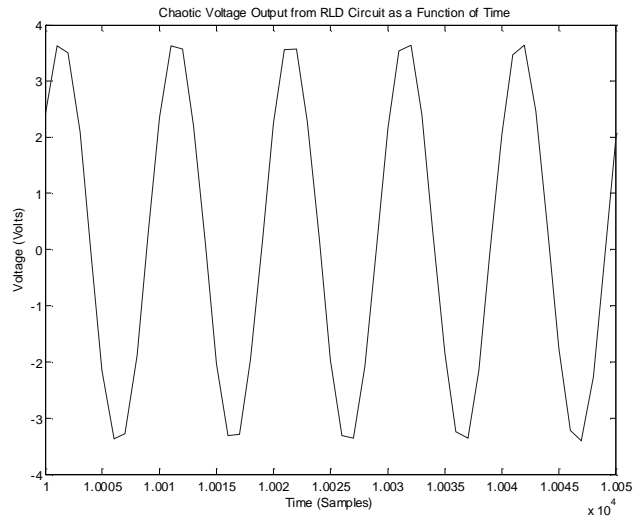
Figure 8.
Time Trace During Chaos. Drive signal: 11.4 V, 20 kHz sine wave.

Viewing the time traces by eye, even while focusing in on a 5 msec segment, was not sufficient for distinguishing among the baseline measurement, periodic orbits, and chaos. We therefore turned to spectral analysis. Signals from the circuit during period doubling, period tripling, and chaos were analyzed as follows.

Spectral Analysis

The data were fast Fourier transformed into the frequency domain for analysis of the spectral components. The coarsest kind of spectral analysis, a basic FFT, revealed strong spectral components at the drive frequency and its harmonics (figure 9).
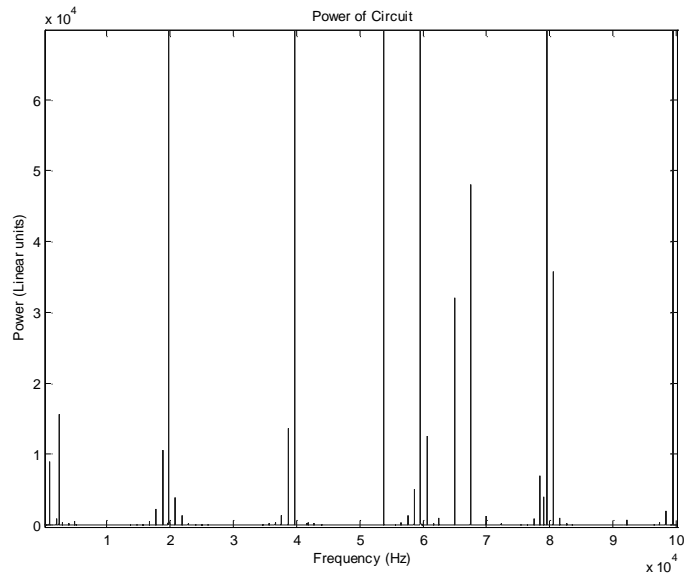
Figure 9.
Linear Power Spectrum of Baseline Voltage Measurement.
Drive signal: 3 V, 20 kHz sine wave.

There were additional peaks at non-harmonic frequencies (such as ~5.5 k Hz) of which we do not know the origin. Close examination of the lowest band revealed a clear 60 Hz source of noise contamination (not shown in detail here).

The most relevant area of the spectrum is the signals at the drive frequency and below. Therefore, the remaining plots only display data up to roughly 20 kHz. Linear plots of the period doubling and period tripling regimes demonstrate spectral components at half and thirds of drive frequency, respectively (figures 10 and 11).
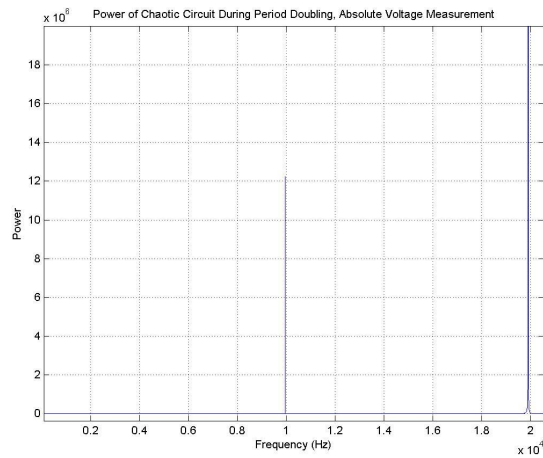
Figure 10.
Linear Power Spectrum of Period Doubling Regime.
Drive signal: 4.9 V, 20 kHz sine wave.
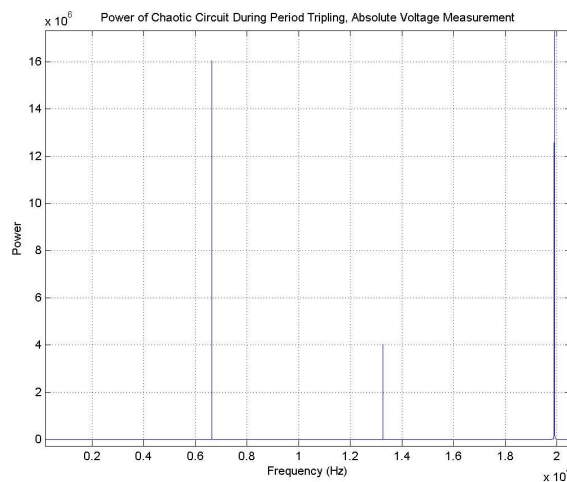
Figure 11.
Linear Power Spectrum of Period Tripling Regime.
Drive signal: 9.1 V, 20 kHz sine wave.

The FFT calculation confirmed that the circuit was behaving as expected, which is demonstrated by the linear-linear power spectrum plots. In the case of period doubling, a sharp spectral component is apparent at the drive frequency and also at half the drive frequency. During the period tripling regime, sharp spectral components appeared at the drive frequency f, 1/3 f, and 2/3 f. Harmonics of the signal are also clearly demonstrated.

The amplitude scale upon which the signal is changing is almost invisible in the linear plots. We therefore plot the spectra in log-linear coordinates. Upon closer examination with log-linear plots, however, it is clear that the data require some processing to remove spectral artifacts. Figure 12 displays an example averaged spectrum plot of period doubling. Spectral plots for all circuit regimes were then recalculated using Welch's method, tapered with a Hanning filter and averaged over 10 segments. Welch's method allows for the averaging out of artifactual spectral components based on the particular taper chosen, and increases the signal to noise ratio within the spectra. Figures 12 through 15 illustrate the power spectra calculated as such under the five drive voltage conditions.
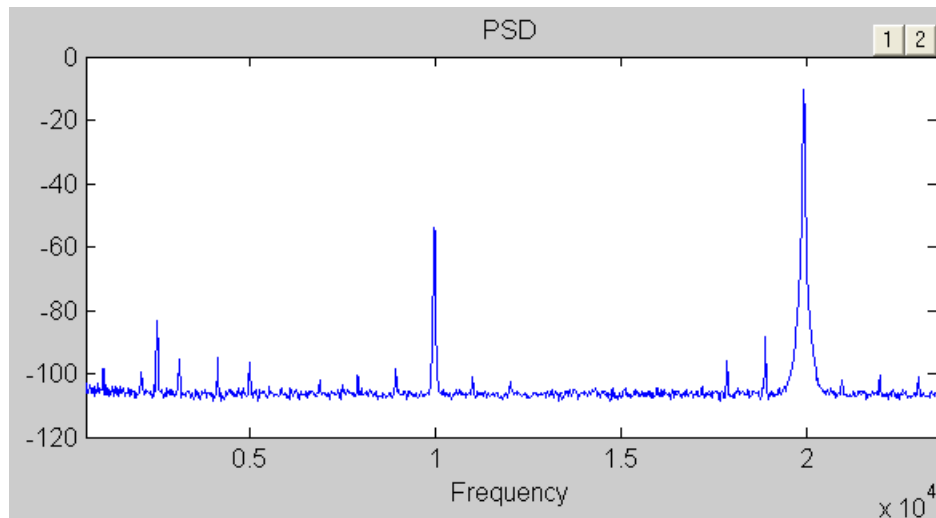
Figure 12.
Average Power Spectrum of Period Doubling Regime.
Drive signal: 3V, 20 kHz sine wave.

Spectra calculated as such were sufficiently clean to make some conclusions about the data. However, it should be noted that a more accurate spectral estimation could be made with overlapping Welch segments. Even better than Welch's method is the multi-taper method, whereby multiple tapers are averaged together to cancel out noise, improving the signal to noise ratio. A further benefit of the multi-taper method is that it enables determination of confidence intervals of the spectral estimates.
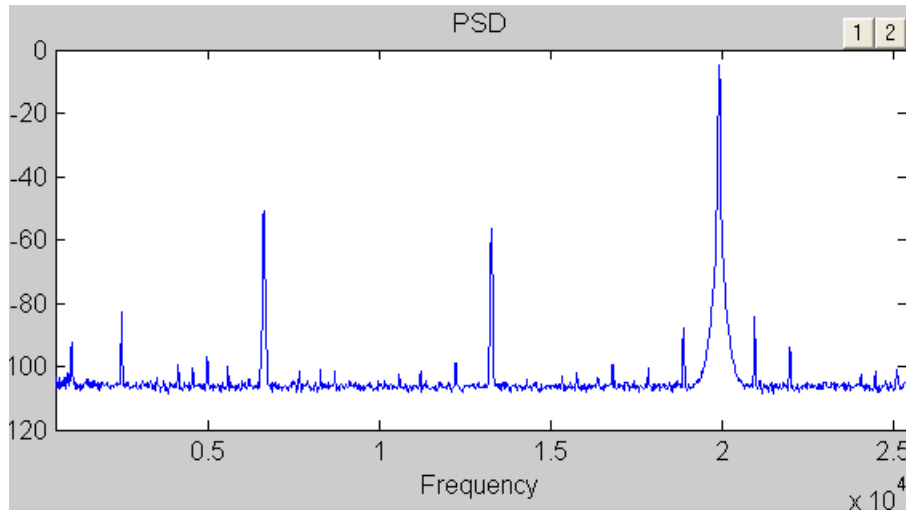
Figure 13.
Average Power Spectrum of Period Tripling Regime.
Drive signal: 9.1 V, 20 kHz sine wave.

Figures 12 and 13 more clearly demonstrate the period doubling and tripling described above, and give a baseline measure of the amount of noise, for comparison with the chaotic regime. The tapered and averaged power spectrum from the chaotic data is demonstrated in figure 14.
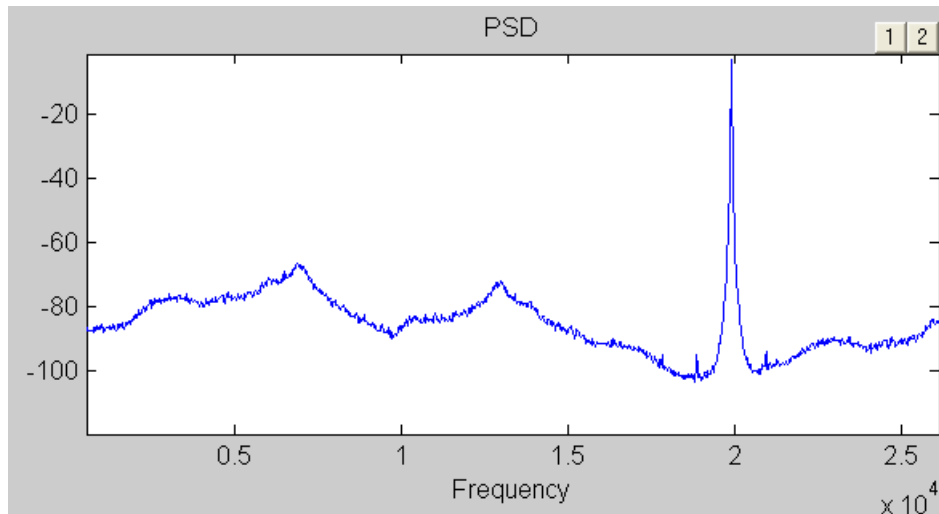
Figure 14.
Average Power Spectrum of Second Chaotic Regime.
Drive signal: 11.4 V, 20 kHz sine wave.

The spectrum of the chaos signal is broadband, as is expected from the definition of chaos. It is also worth noting that the spectrum has strong frequency components at the period tripled frequency values. This is not surprising, given that this particular chaotic regime occurred at a drive voltage just slightly higher than the drive voltage that produced period tripling. The system should therefore favor that attractor.

Phase Space Reconstructions of Time Series Data

The next step in the analysis was to visualize the data in phase space. Our initial guess about an appropriate time lag, τ, was 10 given that there were 10 data points sampled per cycle of the drive signal. The following three plots display 3-dimensional plots of the the time series data for period doubling, period tripling, and chaos based on time lags of 10 and 20.
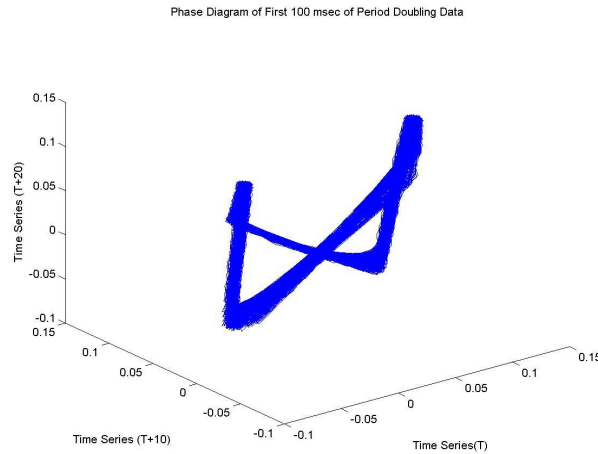
Figure 15.
Phase Space Reconstruction of Period Doubling Data

The period doubling phase diagram displays a fixed periodic orbit that appears to be unfolded in three dimensions.
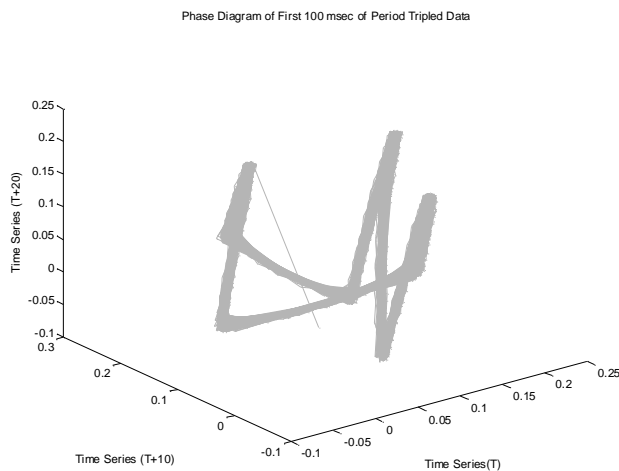
Figure 16.
Phase Space Reconstruction of Period Tripling Data

The period tripling phase plot is slightly more complex than the period doubling phase diagram. It crosses itself a greater number of times, but conserves the overall shape of the period doubling data.
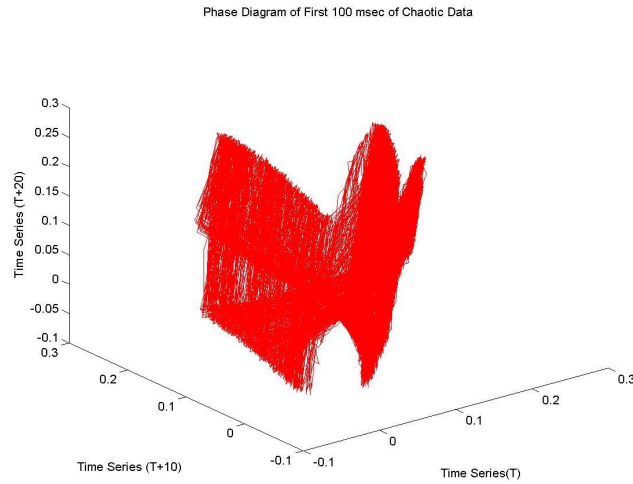
Figure 17.
Phase Space Reconstruction of Chaotic Data

The chaotic phase plot displays the same overall shape as the period tripling data, but is significantly more complex. The plot suggests the aperiodicity of the data because the orbit does not repeat, and thereby fills in the space.

False Nearest Neighbor Analysis of Circuit Data

The plots above were an initial pass at phase space reconstruction based on intuition (dimensionality d = 3 and time lag = 10). The next step in the analysis was to try to determine the correct dimensionality of the chaotic data and plot its attractor. We used the CSPW software and average mutual information metric method described previously to determine the appropriate time lag, τ, for embedding the data into a higher dimension.
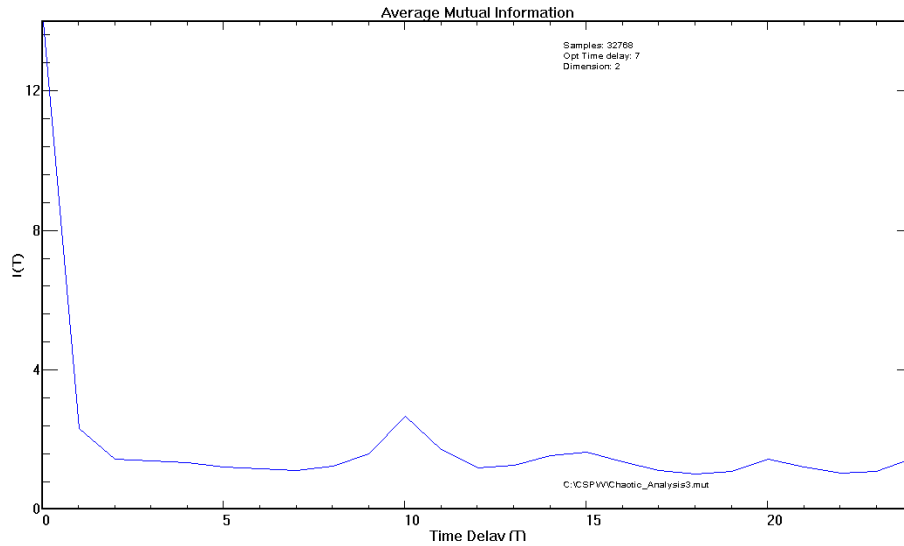
Figure 18.
Average Mutual Information of Chaotic Data

The average mutual information calculation yielded 2 as the intial minimum, suggesting that a time lag of two data steps is appropriate for replotting the time series data in multi-variate space. Surprisingly, the plot also reveals that 10 is a particularly inappropriate value for the time lag because the average mutual information has a local maximum at a time delay of 10.

We then used the software to calculate the percentage of false nearest neighbors as a function of dimension. We set the number of nearest neighbors to be used in the calculation of global distance to be 40, and set a maximum dimension of 20.

The first minimum on this plot suggests that the chaotic data are 3-dimensional (figure 19). A dimensionality of 3 is not surprising considering that our circuit is a modification of a known 3-dimensional nonlinear system, namely, the RLC circuit.
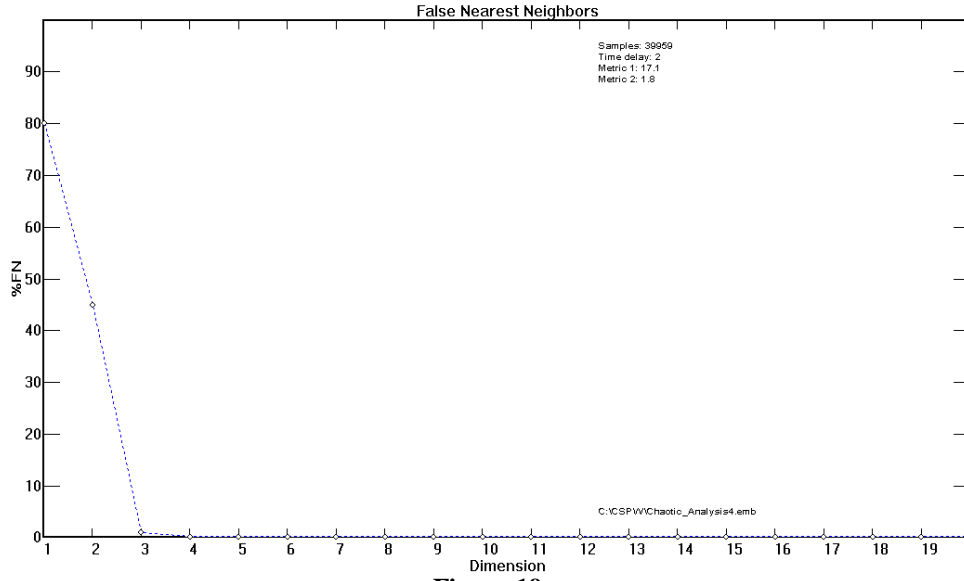
Figure 19.
Dimension Calculation of Chaotic Attractor

Reconstructed Attractors

Finally, we used the CSPW software to plot the underlying attractor of the chaotic data based on the average mutual information and false nearest neighbors analysis described above. The data is best visualized when a subset of the total data points are plotted.

The following three plots are the same attractor, viewed from three different vantage points, based on the first 1000 data points in the sample. If the data is stationary, then it does not matter which 1000 data points are used to create the plot; the results should be the same. We examined the data in a frequency versus time plot to test for stationarity (not illustrated here), and it confirmed that the chaotic data is in fact stationary.
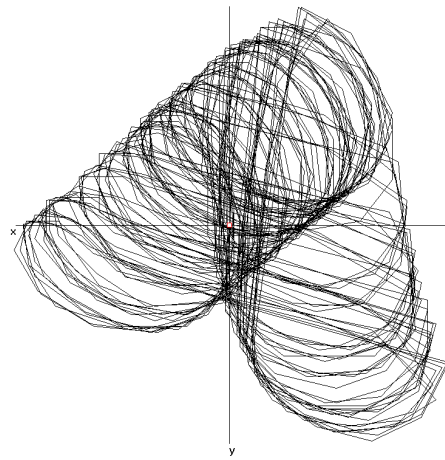
Figure 20 a.
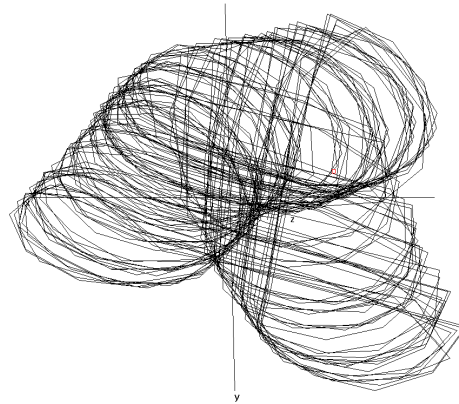
Figure 20 b.
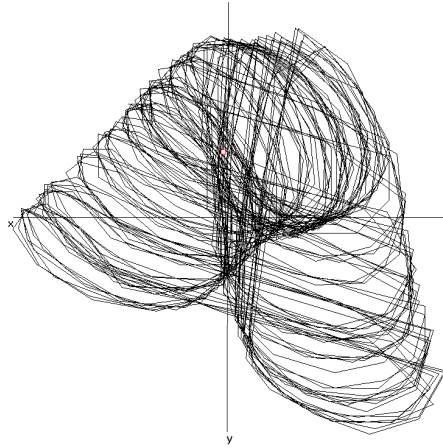
Figure 20 c.

Despite our having embedded the data in a phase space based on a less than ideal time lag, our three dimensional phase plot of chaos (figure17) bears striking resemblance with the attractor depicted here.

This analysis demonstrates that the chaotic behavior of the circuit is described by a three-dimensional system of nonlinear equations.

Preliminary Synchronization Results

Using the circuit as described, synchronization was only possible in non-chaotic regimes. In addition, synchronization was only possible ~10% of the time. Depending upon the initial state of the two resonators, partial synchronization was possible. To change the initial state of the resonators touching resistor R20 injects a large amount of noise, and a small percentage of the time the circuits will be synchronized when the finger is released. Even when the circuits synchronize, when looking at a phase space plot (master vs. slave), the plot is not a straight line. Instead the plot is an orbit; however the number of orbits is reduced when the circuit is "synchronized" vs. when it is not, when there has been one or more bifurcations. This incomplete synchronization would suggest that our unidirectional control circuit is not working correctly. We attribute the main problem to be the phase lag introduced by the opamps, it would be advisable to use opamps with a higher gain than the TL071CN, which would reduce the lag.

To demonstrate that partial synchronization was achieved, we have plotted below the log amplitude of different frequencies from the Master resonator vs. the Slave resonator, shown below. In the unsynchronized case, the frequency amplitudes are less matched to one another than in the synchronized case (not close to an Y=X line). The data was collected at 100 KHz from both Master and Slave resonators; however the corresponding data point in the slave was taken 5ms after that in the master. This means that slave's data is 10% out of phase relative to the master, and thus plotting master vs. slave for pure amplitudes, was never a straight line. In the pure amplitude plot, unsynchronized and synchronized data was indistinguishable from each other.

Unsynchronized   Synchronized
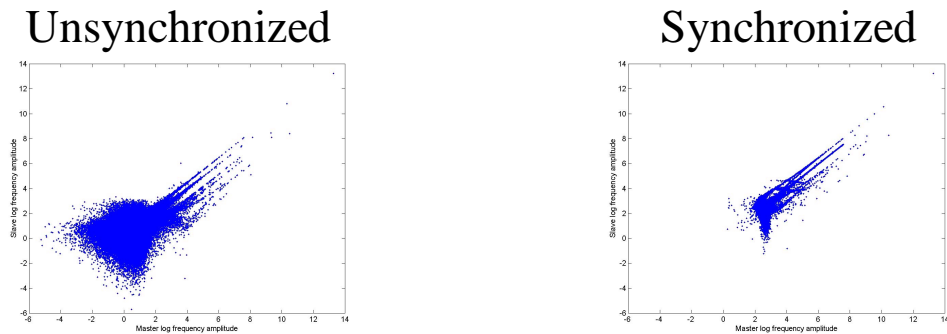
Figure 21.
Comparison of Unsynchronized and Synchronized Circuits

Summary and Conclusions

With a resistor, resistor, diode and inductor in series and a sinusoidal drive signal, we were able to reproduce Lindsay's result and drive a circuit into chaos. Our circuit recapitulated the Feigenbaum universal constant and was very close to the expected value. Our time series analysis, spectral analysis, and phase space embedding demonstrated period doubling and tripling on the route to chaos. Using false nearest neighbor analysis, we calculated the dimensionality of the chaotic data to be 3, based on 40 nearest neighbors and a maximum dimension set at 20. Additionally, we attempted to reproduce synchronization experiments and demonstrated with preliminary data that synchronization of chaotic circuits is possible. Finally, we discuss a few modifications to the circuit that might be interesting to investigate further, including using LEDs and photodiodes.

References

Abarbanel, HDI. Analysis of Observed Chaotic Data. Springer-Verlag, New York 1996.

CSPW Demo software, Version 1.2, 1998.

Elson, RC, Selverston, AI, Huerta, R, Rulkov, NF, Rabinovich, MI, Abarbanel, HDI. Synchronous behavior of two coupled biological neurons. (1998). Physical Review Letters, 81(25): 5692-5695.

Feigenbaum, M.J. (1978). Quantitative universality for a class of nonlinear transformations. Journal of Statistical Physics, 19(1), 25-30.

Greene, M., Paniza, J., Anderson, D. Noise-Induced Behavior in Chaotic Systems: The Logistic Parabola and the L-R-Diode Circuit, Harvard University, Department of Physics.

Linsay, P.S. (1981). Period doubling and chaotic behavior in a driven anharmonic oscillator. Physical Review Letters, 19, 1349-1352.

Mozdy, E., Newell, T.C., Alsing, P.M., Kovanis, V., Gavrielides, A. (1995). Synchronization and control in a unidirectionally coupled array of chaotic diode resonators. Physical Review E., 51(6), 5371-5376.

Newell, T.C., Alsing, P.M., Gavrielides, A., Kovanis, V., Synchronization of chaos using proportional feedback. Physical Review E., 49(1), 313-318.

Oppenheim, A.V. and Schafer, R.W. Discrete-Time Signal Processing, 2nd Ed. Prentice Hall, New Jersey, 1999. Chapter 7, Filter Design Techniques, pp.439-540.

Schaffer, C.B., Classical Chaos, Harvard University, Department of Physics.

Smith, D. (1992). How to generate chaos at home Scientific American, January, 144-146.

Strogatz, S. H. Nonlinear Dynamics and Chaos. Perseus Publishing, Cambridge, 1994.